

Quantum State Preparation and Protection by Measurement-Based Feedback Control Against Decoherence*

YAN Yan (闫妍), ZOU Jian (邹健),[†] WANG Lu (王璐), XU Bao-Ming (徐宝明), WANG Chao-Quan (王朝全), and SHAO Bin (邵彬)

School of Physics, Beijing Institute of Technology, Beijing 100081, China

(Received July 31, 2014; revised manuscript received December 3, 2014)

Abstract We consider an open quantum system subjected to a noise channel under measurement-based feedback control and two prototypical classes of decoherence channels are considered: phase damping and generalized amplitude damping. Based on quantum trajectory theory, we obtain an extended master equation for the dynamics of the reduced system in the presence of feedback control. For a qubit system we analytically solve this master equation and obtain the solution of the state vector dynamics. Then we propose an effective feedback control scheme for preparing an arbitrary quantum pure state. We also study how to protect two nonorthogonal states effectively, and find that projective measurement with unbiased basis is not optimal for this task, while weak measurement with biased basis could realize the best protection of two nonorthogonal states. Furthermore, the inefficiencies in the feedback process are also discussed.

PACS numbers: 03.67.Pp, 03.65.Ta, 02.30.Yy

Key words: quantum feedback control, weak measurement, state preparation, state protection

1 Introduction

Realistic quantum systems always interact with surrounding environment, and the dynamics of such open system is very important in many areas of physics.^[1] In general, open system dynamics cannot be described by the Schrödinger equation, so investigating the reduced system dynamics is a highly nontrivial problem. Various approaches have been developed, and the most common one is the master equation.^[2] The basic idea is to consider the total system consisting of the system of interest and the environment as a closed one, which hence can be solved by using the usual unitary time evolution. The environment degrees of freedom can then be eliminated to obtain a differential equation that only describes the system dynamics. Generally there are two types of decoherence channels which are widely used: phase damping (PD) channel and amplitude damping (AD) channel.^[3] The PD channel describes a decoherence process which is caused by random phase shifts of the system due to its interaction with the environment. The AD channel describes the process in which the initial state will gradually decay to a steady state related to the temperature of the environment.

In the past few years quantum measurement and feedback control have been widely studied. The general framework for quantum feedback was introduced by Wiseman and Milburn^[4–5] who considered the measured photocurrent directly modulating the system Hamiltonian. Relevant experimental achievements^[6–8] have also been obtained. Quantum feedback for continuously monitored systems has been shown to be useful for controlling the state of a quantum system^[4–5,9–16] and improving parameter estimation by adaptive measurement.^[17–19]

Recently, quantum state preparation and protection against decoherence have been the subject of many studies in quantum information processing. Generally, in quantum information processing the system states should be initially prepared in pure states.^[20–21] Because of environmental noise, such open systems often exist naturally in mixed states, and it is necessary to purify them. The majority of work in the field of state purification has been based on “open-loop” control methods, such as algorithmic cooling^[22–24] and dissipation engineering.^[25–26] Also, some authors^[27–30] combined continuous measurement with quantum feedback (or closed-loop) to control the purification process. On the other hand, it is well known that nonorthogonal qubit states are particularly important in the well-known B92 quantum key distribution protocol.^[31] They serve as the simplest set of inputs demonstrating the limitation imposed by quantum measurement: if a system is prepared in one of several nonorthogonal states, no measurement can determine which preparation occurred with certainty.^[32–33] Especially in the presence of noise, the protection of nonorthogonal states becomes a big challenge.^[34] Some measurement and feedback control schemes have been proposed to protect nonorthogonal states against decoherence. To be specific, in Ref. [33], Brańczyk *et al.* investigated how to use measurement and feedback control to protect the state of a qubit. The qubit they considered is prepared in one of two nonorthogonal states in the x - z plane of the Bloch sphere and subjected to noise. In a simple quantum control scenario, Ref. [32] experimentally explored the use of weak measurements in feedback control to stabilize nonorthogonal states of a

*Supported by the National Natural Science Foundation of China under Grant Nos. 11274043 and 11375025

[†]Corresponding author, E-mail: zoujian@bit.edu.cn

qubit against dephasing. Furthermore, Yang *et al.*^[34] extended the scheme to a wide range of initial states and generalized the scheme from earlier works. It is worth noting that in all the state-protection schemes proposed above, they used the Kraus operators to stand for the noise and the feedback control was in the form of a control map. While Ref. [35] derived a master equation to describe the evolution of the whole system consisting of the quantum system and its phase damping environment under measurement-based direct quantum feedback control. Using an approximate method, the density matrix of the system was numerically calculated and the state preparation and protection of the quantum system were discussed.

In this paper, we consider an open quantum system subjected to a noise channel under measurement-based feedback control and two prototypical classes of decoherence channels are considered: phase damping and generalized amplitude damping. Based on quantum trajectory theory,^[36] we obtain an extended master equation for the dynamics of the system under measurement and feedback control. We take a two-level system as an example, and obtain the exact analytic solution of the state vector dynamics. As an application of our explicit form of the state vector dynamics, we propose a simple and effective measurement-based feedback control scheme which can drive any initial states to an arbitrary quantum pure state. We also consider a qubit prepared in one of two nonorthogonal states and subsequently subjected to noise. Our task is to use feedback control to recover it with high fidelity. We demonstrate that projective measurement with unbiased basis is not always optimal for this task, which was usually used in the previous work. And we find that a feedback scheme based on weak measurement with biased basis could realize the best stabilization of two nonorthogonal states. Furthermore, the unavoidable imperfections that may occur in realistic experimental implementations are also taken into account in our discussion.

The paper is organized as follows. Based on quantum trajectory theory, we obtain an extended measurement-based feedback control master equation for an open system in Sec. 2. In Sec. 3, we consider quantum state preparation for a two-level system and analytically obtain the solutions of the state vector dynamics for two kinds of noise channels respectively. In particular, Subsec. 3.1 is devoted to the case of phase-damping channel while Subsec. 3.2 deals with similar analytical studies of state preparation under the amplitude-damping channel. More details about protecting two nonorthogonal states are given in Sec. 4. We discuss the feedback inefficiencies in Sec. 5. And finally, we provide the summary in Sec. 6.

2 An Extended Measurement-Based Feedback Control Master Equation for an Open System

In this section, we try to find an extended master equation describing an open quantum system under measurement and feedback control by using quantum trajectory

theory. A Markovian dynamics can be described by a time-local master equation,^[2,37] and the state density matrix of a Markovian quantum system satisfies the following Lindblad equation^[38]

$$\frac{d}{dt}\hat{\rho}(t) = -\frac{i}{\hbar}[\hat{H}, \hat{\rho}(t)] + \mathcal{L}(\hat{\rho}(t)). \quad (1)$$

The Hermitian operator \hat{H} describes the coherent part of the quantum evolution. The superoperator $\mathcal{L}(\hat{\rho}(t))$ stands for the decoherent part of the quantum evolution, which can be expressed in terms of a collection of (in general non-Hermitian) operators \hat{L}_a (the Lindblad operators) as

$$\mathcal{L}(\hat{\rho}(t)) := \sum_a \left[\hat{L}_a \hat{\rho}(t) \hat{L}_a^\dagger - \frac{1}{2}(\hat{L}_a^\dagger \hat{L}_a \hat{\rho}(t) + \hat{\rho}(t) \hat{L}_a^\dagger \hat{L}_a) \right]. \quad (2)$$

The difference between closed quantum systems and open quantum systems is that the dynamics of open quantum systems contains both unitary part and decoherent part, while the dynamics of closed quantum systems contains only unitary part.

By implementing sequential measurements and feedback controls conditioned on the outcomes of the measurements, one can achieve the goal of manipulating quantum systems. In this paper, we choose a set of POVM measurement operators $\{\hat{M}_j\}$ which satisfies the completeness condition $\sum_j \hat{M}_j^\dagger \hat{M}_j = \hat{I}$. Suppose the measurements occur instantaneously and randomly with an average rate R . After each measurement, we subsequently perform an instantaneous feedback unitary rotation \hat{F}_j conditioned on the measurement result. We consider a time interval Δt which is short enough so that only a single measurement as well as the corresponding feedback can occur with the probability being $R \Delta t$.^[39]

If a measurement does occur, based on the measurement outcome j , we perform a feedback operation \hat{F}_j on the system. Then the density operator becomes:

$$\hat{\rho}_s(t) \rightarrow \hat{\rho}_s(t + \Delta t) = \sum_j (\hat{F}_j \hat{M}_j) \hat{\rho}_s(t) (\hat{F}_j \hat{M}_j)^\dagger. \quad (3)$$

If no measurement occurs and Δt is sufficiently small, we may evaluate this change to the lowest order in Δt :

$$\begin{aligned} \hat{\rho}_s(t) &\rightarrow \hat{\rho}_s(t + \Delta t) \\ &= \hat{\rho}_s(t) - \frac{i}{\hbar}[\hat{H}, \hat{\rho}_s(t)]\Delta t + \mathcal{L}(\hat{\rho}_s(t))\Delta t. \end{aligned} \quad (4)$$

Adding both the measurement-based feedback part and the no-measurement evolution part, weighted by their probability of occurrence, we can obtain the average evolution of the system. To the lowest order in Δt , it is straightforward calculated

$$\begin{aligned} \hat{\rho}_s(t + \Delta t) &= (1 - R\Delta t)\hat{\rho}_s(t) - \frac{i}{\hbar}[\hat{H}, \hat{\rho}_s(t)]\Delta t \\ &\quad + \mathcal{L}(\hat{\rho}_s(t))\Delta t + R\Delta t \sum_j (\hat{F}_j \hat{M}_j) \hat{\rho}_s(t) (\hat{F}_j \hat{M}_j)^\dagger. \end{aligned} \quad (5)$$

We then obtain the master equation by taking the limit $\Delta t \rightarrow 0$,

$$\dot{\hat{\rho}}_S(t) = -\frac{i}{\hbar}[\hat{H}, \hat{\rho}_S(t)] + \mathcal{L}(\hat{\rho}_S(t)) + R\left[\sum_j (\hat{F}_j \hat{M}_j) \hat{\rho}_S(t) (\hat{F}_j \hat{M}_j)^\dagger - \hat{\rho}_S(t)\right]. \quad (6)$$

The first term on the right-hand side is the Liouvillian superoperator, which stands for the unitary portion of the propagation, while the second term, the Lindbladian superoperator, represents the decoherent part of the system. It is noted that the third term represents the measurement-based feedback dynamics, which can also be written in the Lindblad form

$$R\left[\sum_j (\hat{F}_j \hat{M}_j) \hat{\rho}_S(t) (\hat{F}_j \hat{M}_j)^\dagger - \hat{\rho}_S(t)\right] = \sum_j \left(\hat{L}_j \hat{\rho}_S(t) \hat{L}_j^\dagger - \frac{1}{2} \{ \hat{L}_j^\dagger \hat{L}_j, \hat{\rho}_S(t) \} \right), \quad (7)$$

with $\hat{L}_j = \sqrt{\bar{R}} \hat{F}_j \hat{M}_j$. In our approach, both the dissipator induced from the environment and the action of the measurement-based feedback control are in the Lindblad form. The measurement-based feedback control master equation for an open system can be rewritten in a more concise form

$$\frac{d}{dt} \hat{\rho}(t) = -\frac{i}{\hbar} [\hat{H}, \hat{\rho}(t)] + \tilde{\mathcal{L}}(\hat{\rho}(t)), \quad (8)$$

where

$$\tilde{\mathcal{L}}(\hat{\rho}(t)) = \sum_{n=a,j} \left[\hat{L}_n \hat{\rho}(t) \hat{L}_n^\dagger - \frac{1}{2} (\hat{L}_n^\dagger \hat{L}_n \hat{\rho}(t) + \hat{\rho}(t) \hat{L}_n^\dagger \hat{L}_n) \right], \quad (9)$$

and the subscript a stands for the decoherent part and j stands for the measurement-based feedback control part.

3 Quantum State Preparation-Exact Solutions

In this and the following sections, we consider a two-level quantum system, which is the simplest system involving many fundamental features of quantum coherence. Such systems are important in their own right as the elementary carriers of quantum information.^[40–42] In addition, some two state models admit exact solutions. The latter is very useful because it allows one to gain valuable insight into general properties of decoherence and can serve as a step toward consistent approximations for more complicated open systems. In this section for a two-level quantum system, we will employ the master equation obtained in the previous section to show that we can prepare an arbitrary given pure state from any initial states, by using appropriate measurement-based feedback control scheme.

The Hamiltonian of a two-level system is in the following form

$$\hat{H}_S = \hbar \omega_0 \hat{\sigma}_z \quad (10)$$

where ω_0 is the Rabi frequency and $\hat{\sigma}_z$ is the Pauli operator. Without losing generality, we choose an arbitrary target pure state which can be written as

$$|\psi\rangle_{\text{target}} = \cos \frac{\eta}{2} |0\rangle + e^{i\zeta} \sin \frac{\eta}{2} |1\rangle,$$

with $\eta \in [0, \pi]$ and $\zeta \in [0, 2\pi]$. Our goal is to drive the system from any initial state $\hat{\rho}_i$ towards the target pure state $|\psi\rangle_{\text{target}}$ by a proper quantum control scheme. We choose the projective measurements $\hat{M}_+ = |0\rangle\langle 0|$ and $\hat{M}_- = |1\rangle\langle 1|$. Based on the measurement outcomes “ \pm ”, in order to obtain our target state, we perform specific correcting rotations. If the outcome is “ $+$ ”, the corresponding feedback \hat{F}_+ is described as:

$$\begin{aligned} \hat{F}_+ &= \exp\left(-i\zeta \frac{\hat{\sigma}_z}{2}\right) \exp\left(-i\eta \frac{\hat{\sigma}_y}{2}\right) \\ &= \begin{pmatrix} e^{-i\zeta/2} \cos \frac{\eta}{2} & -e^{-i\zeta/2} \sin \frac{\eta}{2} \\ e^{i\zeta/2} \sin \frac{\eta}{2} & e^{i\zeta/2} \cos \frac{\eta}{2} \end{pmatrix}, \end{aligned} \quad (11)$$

and if the outcome is “ $-$ ”, the corresponding \hat{F}_- is described as:

$$\begin{aligned} \hat{F}_- &= \exp\left(-i\zeta \frac{\hat{\sigma}_z}{2}\right) \exp\left(-i(\eta - \pi) \frac{\hat{\sigma}_y}{2}\right) \\ &= \begin{pmatrix} e^{-i\zeta/2} \sin \frac{\eta}{2} & e^{-i\zeta/2} \cos \frac{\eta}{2} \\ -e^{i\zeta/2} \cos \frac{\eta}{2} & e^{i\zeta/2} \sin \frac{\eta}{2} \end{pmatrix}, \end{aligned} \quad (12)$$

where $\hat{\sigma}_y$ and $\hat{\sigma}_z$ are the Pauli operators. From Eqs. (11) and (12), we can see that the feedback \hat{F}_+ (or \hat{F}_-) corresponds to rotating an angle η (or $\eta - \pi$) around the y axis of the Bloch sphere and then an angle ζ around the z axis. The concrete forms of the Lindblad decoherence operators for PD and AD channels and the precise calculations are given in the following two subsections respectively.

3.1 Phase-Damping Channel

Here we consider the phase-damping (PD) channel, which describes a decoherence process caused by random phase shifts of the system due to its interaction with the environment.^[3] The decoherence process is characterized by a single Lindblad operator

$$(\hat{L}_1)_{\text{PD}} = \sqrt{\gamma_{\text{PD}}} \hat{\sigma}_z, \quad (13)$$

where γ_{PD} is the decoherence rate. Let us now apply our extended master equation to study the state preparation by feedback control under this noise channel in more detail.

It is known that a two-level quantum system can also be described by a state vector. The evolution of the state vector is in a more clear form than the state density dynamics in the quantum state preparation problem. Thus we will convert the density matrix into the state vector and obtain the state vector dynamics instead of state density dynamics. Let

$$\hat{\rho} = (1/2)\hat{I} + (1/2)(r_x \hat{\sigma}_x + r_y \hat{\sigma}_y + r_z \hat{\sigma}_z),$$

with the corresponding state vector $\mathbf{r} = (r_x, r_y, r_z)^T$. We suppose that the initial state of the qubit is $\hat{\rho}(t =$

$0) := \hat{\rho}_i = (\hat{\mathbf{I}} + \mathbf{r}_i \cdot \hat{\sigma})/2$ with $\mathbf{r}_i = (r_{ix}, r_{iy}, r_{iz})^T$ and $\hat{\sigma} = (\hat{\sigma}_x, \hat{\sigma}_y, \hat{\sigma}_z)^T$, and the target state is

$$\hat{\rho}_{\text{target}} := |\psi_{\text{target}}\rangle\langle\psi_{\text{target}}| = (\hat{\mathbf{I}} + \mathbf{r}_{\text{target}} \cdot \hat{\sigma})/2$$

with $\mathbf{r}_{\text{target}} = (\sin \eta \cos \zeta, \sin \eta \sin \zeta, \cos \eta)^T$.

In this case, the master equation (Eq. (8)) in Cartesian

coordinates reads as

$$\begin{aligned} \dot{r}_x &= -2\omega_0 r_y + R \cos \zeta \sin \eta - (R + 2\gamma_{\text{PD}})r_x, \\ \dot{r}_y &= 2\omega_0 r_x + R \sin \zeta \sin \eta - (R + 2\gamma_{\text{PD}})r_y, \\ \dot{r}_z &= R(\cos \eta - r_z), \end{aligned} \quad (14)$$

and the solution of Eq. (8) can be obtained

$$\begin{pmatrix} r_x(t) \\ r_y(t) \\ r_z(t) \end{pmatrix} = \begin{pmatrix} A_{11}^{(\text{PD})} & A_{12}^{(\text{PD})} & 0 \\ A_{21}^{(\text{PD})} & A_{22}^{(\text{PD})} & 0 \\ 0 & 0 & A_{33}^{(\text{PD})} \end{pmatrix} \begin{pmatrix} r_{ix} \\ r_{iy} \\ r_{iz} \end{pmatrix} + \begin{pmatrix} B_1^{(\text{PD})} \\ B_2^{(\text{PD})} \\ B_3^{(\text{PD})} \end{pmatrix}, \quad (15)$$

where

$$\begin{aligned} A_{11}^{(\text{PD})} &= \cos(2\omega_0 t) e^{-(R+2\gamma_{\text{PD}})t}, & A_{12}^{(\text{PD})} &= -\sin(2\omega_0 t) e^{-(R+2\gamma_{\text{PD}})t}, \\ A_{21}^{(\text{PD})} &= \sin(2\omega_0 t) e^{-(R+2\gamma_{\text{PD}})t}, & A_{22}^{(\text{PD})} &= \cos(2\omega_0 t) e^{-(R+2\gamma_{\text{PD}})t}, & A_{33}^{(\text{PD})} &= e^{-Rt}, \\ B_1^{(\text{PD})} &= \frac{e^{-(R+2\gamma_{\text{PD}})t} R \sin \eta (R + 2\gamma_{\text{PD}}) [e^{(R+2\gamma_{\text{PD}})t} \cos \zeta - \cos(\zeta + 2\omega_0 t)]}{(R + 2\gamma_{\text{PD}})^2 + 4\omega_0^2} \\ &\quad + \frac{e^{-(R+2\gamma_{\text{PD}})t} R \sin \eta 2\omega_0 [-e^{(R+2\gamma_{\text{PD}})t} \sin \zeta + \sin(\zeta + 2\omega_0 t)]}{(R + 2\gamma_{\text{PD}})^2 + 4\omega_0^2}, \\ B_2^{(\text{PD})} &= \frac{e^{-(R+2\gamma_{\text{PD}})t} R \sin \eta (R + 2\gamma_{\text{PD}}) [e^{(R+2\gamma_{\text{PD}})t} \sin \zeta - \sin(\zeta + 2\omega_0 t)]}{(R + 2\gamma_{\text{PD}})^2 + 4\omega_0^2}, \\ &\quad + \frac{e^{-(R+2\gamma_{\text{PD}})t} R \sin \eta 2\omega_0 [e^{(R+2\gamma_{\text{PD}})t} \cos \zeta - \cos(\zeta + 2\omega_0 t)]}{(R + 2\gamma_{\text{PD}})^2 + 4\omega_0^2}, \\ B_3^{(\text{PD})} &= (-e^{-Rt} + 1) \cos \eta. \end{aligned} \quad (16)$$

From Eqs. (15) and (16), it can be seen that in the long time limit, the matrix $A_{3 \times 3}^{(\text{PD})}$ becomes zero and any initial state vector $\mathbf{r}_i = (r_{ix}, r_{iy}, r_{iz})^T$ can be driven to the state vector $B_{3 \times 1}^{(\text{PD})} = (B_1^{(\text{PD})}, B_2^{(\text{PD})}, B_3^{(\text{PD})})^T$, where $B_{3 \times 1}^{(\text{PD})} \rightarrow (\sin \eta \cos \zeta, \sin \eta \sin \zeta, \cos \eta)^T = \mathbf{r}_{\text{target}}$ (our target state vector) with increasing t .

between two quantum states, and in the Bloch sphere representation, the trace distance between $\hat{\rho}_{\text{target}}$ and $\hat{\rho}(t)$ can be calculated:^[3]

$$D(\hat{\rho}(t), \hat{\rho}_{\text{target}}) = \frac{|\mathbf{r}(t) - \mathbf{r}_{\text{target}}|}{2}. \quad (17)$$

The performances of the preparation protocol for three typical kinds of initial states as examples are shown in Fig. 1. It can be seen clearly that as time evolves, the trace distances between the quantum states at time t and the target state are getting smaller and smaller with increasing t . The steady states are nearly the target state for the trace distances become almost zero in all the three cases, which means that we can realize our goal of preparing an arbitrary given quantum state from any initial states by using our measurement and feedback control under the PD channel. It is worth noting that although the evolutions are different at the beginning for different initial states, afterward, they have the same trends. While, if we do not perform any measurement and feedback control, the system will evolve just under the influence of the environment, and finally it becomes a mixed state. From our calculations, we also find that as the measurement rate R increases, the final state becomes closer to the target state.

3.2 Amplitude-Damping Channel

In this subsection, we consider the generalized amplitude-damping channel described by the Lindblad op-

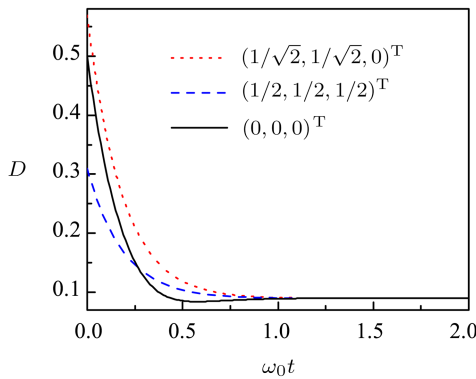


Fig. 1 (Color online) The trace distances as functions of the scaled time $\omega_0 t$ for different initial states \mathbf{r}_i under the PD channel: pure state $\mathbf{r}_i = (1/\sqrt{2}, 1/\sqrt{2}, 0)^T$ (red dotted line), mixed state $\mathbf{r}_i = (1/2, 1/2, 1/2)^T$ (blue dashed line) and maximum mixed state $\mathbf{r}_i = (0, 0, 0)^T$ (black solid line). The other parameters are $\gamma_{\text{PD}} = 0.1$, $R = 5$, $\eta = \pi/6$, $\zeta = 0$.

We use the trace distance as our measure of “closeness”

erators

$$(\hat{L}_1)_{AD} = \sqrt{\frac{\gamma_{AD}}{e^\beta - 1}} \hat{\sigma}_+, \quad (\hat{L}_2)_{AD} = \sqrt{\frac{\gamma_{AD} e^\beta}{e^\beta - 1}} \hat{\sigma}_-, \quad (18)$$

where $\hat{\sigma}_\pm := (\hat{\sigma}_x \pm i\hat{\sigma}_y)/2$, and the non-negative quantities γ_{AD} and β , respectively, describe the decoherence rate and the effective inverse temperature of the environment.

For the AD channel, the master equation in Cartesian

$$\begin{pmatrix} r_x(t) \\ r_y(t) \\ r_z(t) \end{pmatrix} = \begin{pmatrix} A_{11}^{(AD)} & A_{12}^{(AD)} & 0 \\ A_{21}^{(AD)} & A_{22}^{(AD)} & 0 \\ 0 & 0 & A_{33}^{(AD)} \end{pmatrix} \begin{pmatrix} r_{ix} \\ r_{iy} \\ r_{iz} \end{pmatrix} + \begin{pmatrix} B_1^{(AD)} \\ B_2^{(AD)} \\ B_3^{(AD)} \end{pmatrix}, \quad (20)$$

where

$$\begin{aligned} A_{11}^{(AD)} &= \cos(2\omega_0 t) e^{-(1/2)(2R + \gamma_{AD} \coth(\beta/2))t}, & A_{12}^{(AD)} &= -\sin(2\omega_0 t) e^{-(1/2)(2R + \gamma_{AD} \coth(\beta/2))t}, \\ A_{21}^{(AD)} &= \sin(2\omega_0 t) e^{-(1/2)(2R + \gamma_{AD} \coth(\beta/2))t}, & A_{22}^{(AD)} &= \cos(2\omega_0 t) e^{-(1/2)(2R + \gamma_{AD} \coth(\beta/2))t}, \\ A_{33}^{(AD)} &= e^{-(R + \gamma_{AD} \coth(\beta/2))t}, \\ B_1^{(AD)} &= \frac{PQ(e^{Rt + (1/2)\gamma_{AD} \coth(\beta/2)t} \cos \zeta - \cos(\zeta + 2\omega_0 t))}{Q^2 + 16(e^\beta - 1)^2 \omega_0^2} \\ &\quad - \frac{4P(e^\beta - 1)(e^{Rt + (1/2)\gamma_{AD} \coth(\beta/2)t} \sin \zeta - \sin(\zeta + 2\omega_0 t))\omega_0}{Q^2 + 16(e^\beta - 1)^2 \omega_0^2}, \\ B_2^{(AD)} &= \frac{PQ(e^{Rt + (1/2)\gamma_{AD} \coth(\beta/2)t} \sin \zeta - \sin(\zeta + 2\omega_0 t))}{Q^2 + 16(e^\beta - 1)^2 \omega_0^2} \\ &\quad + \frac{4P(e^\beta - 1)(e^{Rt + (1/2)\gamma_{AD} \coth(\beta/2)t} \cos \zeta - \cos(\zeta + 2\omega_0 t))\omega_0}{Q^2 + 16(e^\beta - 1)^2 \omega_0^2}, \\ B_3^{(AD)} &= \frac{e^{-(R + \gamma_{AD} \coth(\beta/2))t} (e^\beta - 1) (e^{(R + \gamma_{AD} \coth(\beta/2))t} - 1) (R \cos \eta - \gamma_{AD})}{e^\beta (R + \gamma_{AD}) - R + \gamma_{AD}}, \\ P &= 2e^{-(1/2)(2R + \gamma_{AD} \coth(\beta/2))t} (e^\beta - 1) R \sin \eta, \quad Q = \gamma - 2R + e^\beta (2R + \gamma). \end{aligned} \quad (21)$$

It can be seen that in the long time limit, the matrix $A_{3 \times 3}^{(AD)}$ becomes zero and the operator $A_{3 \times 3}^{(AD)}$ and $B_{3 \times 1}^{(AD)}$ can transfer an initial state vector $\mathbf{r}_i = (r_{ix}, r_{iy}, r_{iz})^T$ to the state vector

$$\begin{aligned} B_{3 \times 1}^{(AD)} &= (B_1^{(AD)}, B_2^{(AD)}, B_3^{(AD)})^T, \\ B_{3 \times 1}^{(AD)} &\rightarrow (\sin \eta \cos \zeta, \sin \eta \sin \zeta, \cos \eta)^T, \end{aligned}$$

which is exactly our target state vector and is independent of the initial state. This means that we can drive any initial state to the target pure state effectively. The performance of the protocol can also be influenced by β . As it is shown in Fig. 2, the effect of preparation gets better with the increasing of β , i.e., the decreasing of the temperature. It is reasonable because higher temperature will disturb the preparation process as expected. When $\beta \geq 1$, varying β will only lead to small change of the trace distance, which means that as long as the temperature is not high enough, our scheme to prepare an arbitrary pure state under the AD channel is still very effective.

coordinates reads as

$$\begin{aligned} \dot{r}_x &= -2\omega_0 r_y + R \cos \zeta \sin \eta - \left(R + \frac{\gamma_{AD}(1 + e^\beta)}{2(e^\beta - 1)}\right) r_x, \\ \dot{r}_y &= 2\omega_0 r_x + R \sin \zeta \sin \eta - \left(R + \frac{\gamma_{AD}(1 + e^\beta)}{2(e^\beta - 1)}\right) r_y, \\ \dot{r}_z &= R(\cos \eta - r_z) - \gamma_{AD} - \frac{\gamma_{AD}(1 + e^\beta)}{e^\beta - 1} r_z, \end{aligned} \quad (19)$$

and the solution is in the following form

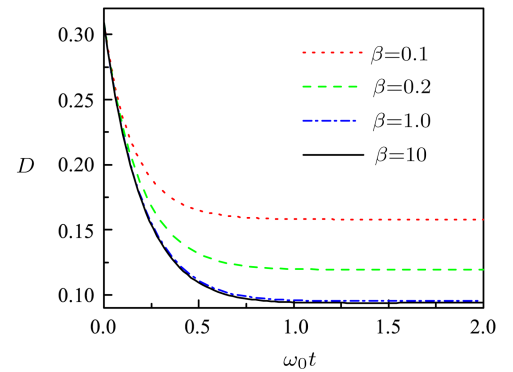


Fig. 2 (Color online) The trace distances as functions of the scaled time $\omega_0 t$ for different β under the AD channel: $\beta = 0.1$ (red dot line), $\beta = 0.2$ (green dashed line), $\beta = 1$ (blue dash dotted line) and $\beta = 10$ (black solid line). The other parameters are $\gamma_{AD} = 0.1$, $R = 5$, $\eta = \pi/6$, $\zeta = 0$, and the initial parameters are $\mathbf{r}_i = (1/2, 1/2, 1/2)^T$.

We plot the trace distances as functions of the scaled time $\omega_0 t$ for different noise channels in Fig. 3. Through

our study, we find that for preparing an arbitrary pure state under two kinds of noise channels, the effect of our measurement-based feedback control scheme under the PD channel is better than that under the AD channel, especially for larger decoherence rates γ_{PD} and γ_{AD} , which stands for severer environment noise (see Figs. 3(a) and 3(b)). We also find that in the long time limit, different initial states as well as target state parameter ζ will not change the trace distance between the steady state and the target state, but varying the measurement rate R and the target state parameter η will have influence on the trace distance. The higher the measurement rate R , the closer between our preparation state and the target state. Besides, we find that our scheme becomes more effective when $\eta \rightarrow 0$.

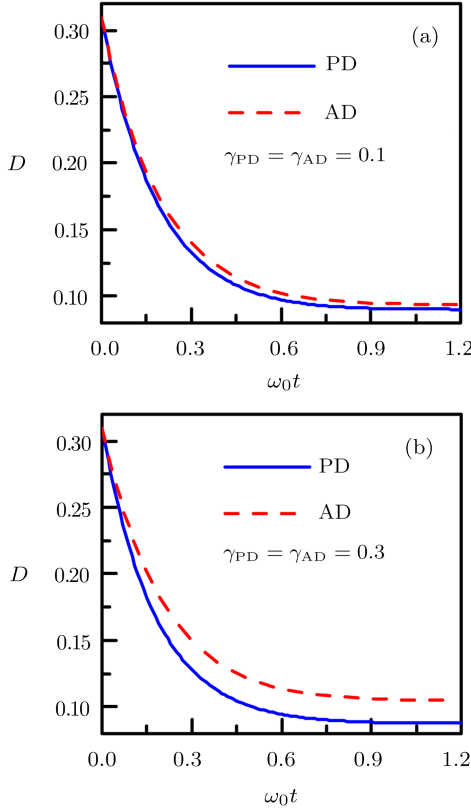


Fig. 3 (Color online) The trace distances as functions of the scaled time $\omega_0 t$ for different noise channels: PD channel (blue solid line) and AD channel (red dashed line). (a) $\gamma_{PD} = \gamma_{AD} = 0.1$; (b) $\gamma_{PD} = \gamma_{AD} = 0.3$. For the AD channel, the temperature of the environment is 0, i.e. $\beta \rightarrow \infty$. The other parameters are $R = 5$, $\eta = \pi/6$, $\zeta = 0$, and the initial parameters are $\mathbf{r}_i = (1/2, 1/2, 1/2)^T$.

4 Protection of Two Nonorthogonal States

Now we consider a qubit prepared in one of two nonorthogonal states, and it is transmitted along a noisy quantum channel. Here we choose two nonorthogonal states because they serve as the simplest set of inputs^[32] demonstrating the limitation imposed by quantum measurement: one can not perfectly discriminate the input

states^[36] and control the resulting (known) input against noise subsequently. Nonorthogonal qubit states are particularly important in the well-known B92 quantum key distribution protocol.^[31] While in this section, our task is that without knowing which state was transmitted, we will attempt to determine which of the two preparations took place and “correct” the system, i.e., undo the effect of the noise, through the use of measurement-based feedback scheme.

In this paper, we consider two general nonorthogonal states $|\psi_+\rangle$ and $|\psi_-\rangle$, which are usually as hypotheses of a standard two-state discrimination problem. By choosing the appropriate orthonormal basis, the two states $|\psi_+\rangle$, $|\psi_-\rangle$ can always be written as

$$|\psi_{\pm}\rangle = \cos \frac{\theta}{2} |+\rangle \pm \sin \frac{\theta}{2} |-\rangle, \quad (22)$$

with $|\pm\rangle = (1/\sqrt{2})(|0\rangle \pm |1\rangle)$. The overlap of the two nonorthogonal states is $\langle\psi_+|\psi_-\rangle = \cos \theta$. The unit vectors $|+\rangle$, $|-\rangle$ are the elements of the basis that span the plane \mathcal{P} formed by $|\psi_+\rangle$, $|\psi_-\rangle$. Two arbitrary orthonormal vectors $|\omega_0\rangle$, $|\omega_1\rangle$ which belong to \mathcal{P} , can be written as

$$\begin{aligned} |\omega_0\rangle &= \cos \frac{\phi}{2} |+\rangle + \sin \frac{\phi}{2} |-\rangle, \\ |\omega_1\rangle &= \sin \frac{\phi}{2} |+\rangle - \cos \frac{\phi}{2} |-\rangle. \end{aligned} \quad (23)$$

The above orthonormal vectors would stand for any projective measurement bases in the plane \mathcal{P} .

We plot a schematic diagram showing the measurement bases and the two nonorthogonal states in Fig. 4. The red dotted line and the green dashed line which can be seen in Fig. 4 stand for the directions of the measurement bases. As is shown that when $\phi = \pi/2$, the measurement basis coincide with z axis, and we call it “unbiased” measurement basis, otherwise it is called “biased” measurement basis. If $\phi = \theta$ or $\phi = \pi - \theta$, we refer to the measurement bases in these two limits as being “fully biased” measurement bases.

In order to find the optimal feedback control scheme, i.e., to minimize the error probability and realize the best recovery, we use the measurement operators in the following forms:

$$\begin{aligned} \hat{M}_+ &= \cos \frac{\chi}{2} |\omega_0\rangle\langle\omega_0| + \sin \frac{\chi}{2} |\omega_1\rangle\langle\omega_1|, \\ \hat{M}_- &= \sin \frac{\chi}{2} |\omega_0\rangle\langle\omega_0| + \cos \frac{\chi}{2} |\omega_1\rangle\langle\omega_1|. \end{aligned} \quad (24)$$

Depending on the choice of the parameter $\chi \in [0, \pi/2]$, one can adjust the measurement strength. When $\cos \chi = 0$, it stands for no measurement and $\cos \chi = 1$ stands for projective measurement, while $0 < \cos \chi < 1$, it is called weak measurement. Reference [43] discussed theoretically about the experimental realization of the weak measurement, and it was realized recently in a photonic architecture.^[32] Based on the measurement outcomes “ \pm ”, we perform specific correcting rotations. If the outcome is “+”, the corresponding feedback \hat{F}_+ is described as:

$$\hat{F}_+ = \exp \left(-i(\phi - \theta) \frac{\hat{\sigma}_y}{2} \right)$$

$$= \begin{pmatrix} \cos \frac{\phi - \theta}{2} & -\sin \frac{\phi - \theta}{2} \\ \sin \frac{\phi - \theta}{2} & \cos \frac{\phi - \theta}{2} \end{pmatrix}, \quad (25)$$

and if “−”, the corresponding \hat{F}_- is described as:

$$\begin{aligned} \hat{F}_- &= \exp \left(-i(\phi + \theta - \pi) \frac{\hat{\sigma}_y}{2} \right) \\ &= \begin{pmatrix} \sin \frac{\phi + \theta}{2} & \cos \frac{\phi + \theta}{2} \\ -\cos \frac{\phi + \theta}{2} & \sin \frac{\phi + \theta}{2} \end{pmatrix}. \end{aligned} \quad (26)$$

From Eqs. (25) and (26), we can see that \hat{F}_+ (or \hat{F}_-) corresponds to rotating around the y axis of the Bloch sphere with a rotation angle $\phi - \theta$ (or $\phi + \theta - \pi$). We attempt to use our measurement and feedback control to protect two nonorthogonal quantum states in either phase-damping or amplitude-damping channel, by considering both biased and unbiased measurement bases, as well as any measurement strength.

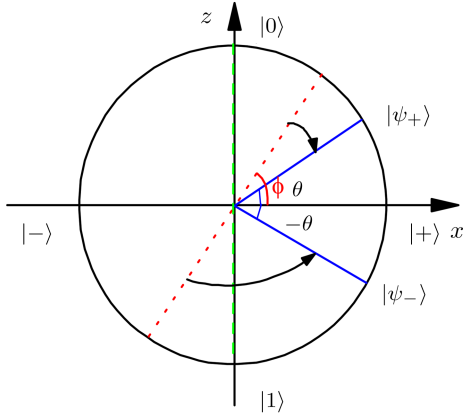


Fig. 4 (Color online) The states $|\psi_+\rangle$ and $|\psi_-\rangle$ are separated by a Bloch-space angle of 2θ (blue solid line). The measurement bases are shown: The red dotted line is referred to as a “biased” measurement basis, and the green dashed line is referred to as an “unbiased” measurement basis.

If q_{\pm} ($q_+ \geq q_-$) is the prior probability of $|\psi_{\pm}\rangle$ being transmitted, to quantify the performance of our protection, we use the average fidelity F between the noiseless input state and the corrected output state as a measure:

$$F = q_+ \sqrt{\langle \psi_+ | \hat{\rho}_+(t) | \psi_+ \rangle} + q_- \sqrt{\langle \psi_- | \hat{\rho}_-(t) | \psi_- \rangle}. \quad (27)$$

The effects of our protection scheme depend on the initial state, and Ref. [44] has shown that the parameter of the “best measurement” basis (see Eqs. (23) and (24)) satisfies:

$$\phi = \arccos \left(\frac{q_+ - q_-}{R_0} \cos \theta \right), \quad (28)$$

where $R_0 = \sqrt{1 - 4q_+q_- \cos^2 \theta}$. In their and our approach, by “best measurement” we mean the measurement that maximizes the probability of discrimination, or equivalently, the one that minimizes the error probability.

For any given two nonorthogonal states from numerical calculations we can find the optimal schemes for biased

measurement basis and unbiased measurement basis, respectively. Generally, the optimal values of the measurement strength parameter χ in Eq. (24) for both biased and unbiased measurement bases are not zero, which means that the weak measurement can better protect the two nonorthogonal states than the projective measurement. Besides, choosing biased measurement basis with condition Eq. (28) (“best measurement” basis) can protect the two nonorthogonal states better (higher fidelity) than the unbiased measurement basis in most cases, in other words, weak measurement with “best-biased basis” can achieve the highest fidelity for our two nonorthogonal states protection.

As an example, we firstly consider that the two nonorthogonal states are $|\psi_{\pm}\rangle = \cos(\pi/10)|+\rangle \pm \sin(\pi/10)|-\rangle$, $q_+ = 0.7$, $q_- = 0.3$ under the PD channel. For these two nonorthogonal states, in Fig. 5 we plot the fidelities as functions of the scaled time $\omega_0 t$ for the following cases: do-nothing (just pass the noise channel without doing anything); the optimal weak measurement with the best-biased basis; projective measurement with the best-biased basis; the optimal weak measurement with unbiased basis; projective measurement with unbiased basis. From Fig. 5, it can be seen that the fidelity decreases rapidly as time evolves for do-nothing. For the unbiased measurement basis, the optimal measurement strength parameter χ is not zero, which means that weak measurement can better protect the two nonorthogonal states than projective measurement, and the optimal value of χ is 0.41; besides, choosing the best-biased measurement basis (see Eq. (28)) can further enhance the fidelity than the unbiased measurement basis, and we also find the optimal value of χ for the best-biased measurement basis, which is $\chi = 0.22$. As shown in Fig. 5 that projective measurement with unbiased basis is not optimal for the protection task, and weak measurement with the best-biased basis can enhance the protective effect. The fidelity improvement by the optimal weak measurement with best-biased basis is better than any other cases.

Now we consider the AD channel. In Fig. 6, we demonstrate the results under the AD channel. As an example, we consider two initial states $|\psi_{\pm}\rangle = \cos(\pi/10)|+\rangle \pm \sin(\pi/10)|-\rangle$ and $q_+ = 0.7$, $q_- = 0.3$. As time evolves, the system will reach its steady state, and the weak measurement with the best-biased basis realizes the optimal recovery from noise than any other protection schemes. With our initial condition under the AD channel, the optimal scheme for weak measurement with the best-biased basis satisfies $\chi = 0.25$ while the optimal weak measure-

ment with unbiased basis satisfies $\chi = 0.41$.

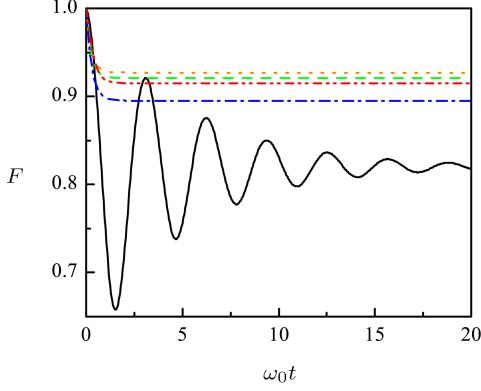


Fig. 5 (Color online) The fidelities as functions of the scaled time $\omega_0 t$ with different measurement-based feedback schemes under the PD channel. The optimal scheme for weak measurement ($\chi = 0.22$) with the best-biased basis (orange dotted line), projective measurement with the best-biased basis (green dashed line), the optimal weak measurement ($\chi = 0.41$) with unbiased basis (red dash-dot-dotted line), projective measurement with unbiased basis (blue dash-dotted line) and without any measurement and operation (black solid line). The initial parameters are $\theta = \pi/5$, $q_+ = 0.7$, $q_- = 0.3$. $R = 8$, $\gamma = 0.1$.

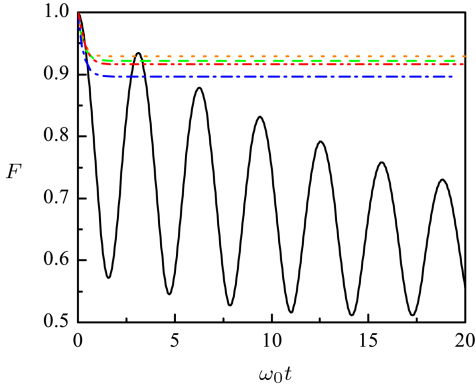


Fig. 6 (Color online) The fidelities as functions of the scaled time $\omega_0 t$ with different measurement-based feedback schemes under the AD channel. The optimal scheme for weak measurement ($\chi = 0.25$) with the best-biased basis (orange dotted line), projective measurement with the best-biased basis (green dashed line), the optimal weak measurement ($\chi = 0.41$) with unbiased basis (red dash-dot-dotted line), projective measurement the unbiased basis (blue dash dot line) and without any measurement and operation (black solid line). The initial parameters are $\theta = \pi/5$, $q_+ = 0.7$, $q_- = 0.3$. The temperature of the environment is 0, i.e. $\beta \rightarrow \infty$. $R = 8$, $\gamma = 0.1$.

It is worth noting that for do-nothing just pass the PD channel, there is a damped oscillation for the system and it finally evolves into a steady state whose fidelity is always higher than that just under the AD channel. The AD channel describes the process in which the initial state will gradually decay to the ground state for zero temperature, so the fidelity between the initial state and the steady state

is much lower. From our study, we find that for the same initial condition with $\theta \rightarrow 0$ ($\theta = 0$ corresponds to the two nonorthogonal states overlapping completely, and along x-axis), the fidelity of the protection scheme under the AD channel is a little higher than that under the PD channel. For the PD channel, when q_+ is close to 1 (q_- is close to 0), we could always find protection schemes using our measurement-based feedback control; besides, if q_+ is close to q_- , we can also find proper protection schemes better than do-nothing in most cases except for $\theta \rightarrow \pi/2$. That is because when $\theta \rightarrow \pi/2$, which is nearly the eigenstates of $\hat{H}_S = \hbar\omega_0\hat{\sigma}_z$, the PD channel with $(\hat{L}_1)_{PD} = \sqrt{\gamma_{PD}}\hat{\sigma}_z$ is not detrimental to the two nonorthogonal states. For the AD channel, we can always find some measurement-based feedback control schemes which can enhance the fidelity than do-nothing. Considering the amount of increase between our optimal measurement-based feedback scheme and do-nothing, our schemes under the AD channel have better protective effect than that under the PD channel.

5 Feedback Inefficiencies Effects

Up to now, our discussion has neglected the effects of inefficiencies in the feedback process, which are important in realistic experimental implementations. Since the feedback relies on the outcomes of the measurement, it is reasonable to consider the case in which a measurement does not cause a feedback. The extension of the master equation (6) to allow for finite efficiency can be obtained by adding the situation when a measurement does occur but there is no feedback:

$$\hat{\rho}_s(t) \rightarrow \hat{\rho}_s(t + \Delta t) = \sum_j \hat{M}_j \hat{\rho}_s(t) \hat{M}_j^\dagger, \quad (29)$$

with the probability being $(1 - p)R\Delta t$.

While, as in the perfect feedback case, if a measurement does occur and the corresponding feedback operation \hat{F}_j is applied on the system:

$$\hat{\rho}_s(t) \rightarrow \hat{\rho}_s(t + \Delta t) = \sum_j (\hat{F}_j \hat{M}_j) \hat{\rho}_s(t) (\hat{F}_j \hat{M}_j)^\dagger, \quad (30)$$

with the probability being $pR\Delta t$. If no measurement occurs:

$$\begin{aligned} \hat{\rho}_s(t) &\rightarrow \hat{\rho}_s(t + \Delta t) \\ &= \hat{\rho}_s(t) - \frac{i}{\hbar} [\hat{H}, \hat{\rho}_s(t)] \Delta t + \mathcal{L}(\hat{\rho}_s(t)) \Delta t, \end{aligned} \quad (31)$$

with the probability being $1 - R\Delta t$. Adding all the above parts and weighted by their probability of occurrence, we can obtain the master equation considering the inefficiencies of feedback

$$\begin{aligned} \dot{\hat{\rho}}_s(t) &= -\frac{i}{\hbar} [\hat{H}, \hat{\rho}_s(t)] + \mathcal{L}(\hat{\rho}_s(t)) \\ &+ R \left[p \sum_j (\hat{F}_j \hat{M}_j) \hat{\rho}_s(t) (\hat{F}_j \hat{M}_j)^\dagger \right. \\ &\left. + (1 - p) \sum_j \hat{M}_j \hat{\rho}_s(t) \hat{M}_j^\dagger - \hat{\rho}_s(t) \right]. \end{aligned} \quad (32)$$

When the feedback efficiency $p = 0$, there is no feedback control and only measurement performs on the system. Evidently, for a perfect feedback process $p = 1$, Eq. (6) is regained. In the intermediate case where $0 < p < 1$, one would expect that not all corresponding feedbacks are applied after measurements which lead to an inefficient control. Due to the lack of efficient feedback after measurement, the effects of preparing and protecting quantum states are getting worse. We take the

preparation of an arbitrary pure state in the PD noise as an example. In this case, the master equation (Eq. (32)) in Cartesian coordinates reads as

$$\begin{aligned}\dot{r}_x &= -2\omega_0 r_y + pR \cos \zeta \sin \eta - (R + 2\gamma_{PD})r_x, \\ \dot{r}_y &= 2\omega_0 r_x + pR \sin \zeta \sin \eta - (R + 2\gamma_{PD})r_y, \\ \dot{r}_z &= pR(\cos \eta - r_z),\end{aligned}\quad (33)$$

and the solution of Eq. (33) can be obtained

$$\begin{pmatrix} r_x(t) \\ r_y(t) \\ r_z(t) \end{pmatrix} = \begin{pmatrix} A_{11}^{(PD)} & A_{12}^{(PD)} & 0 \\ A_{21}^{(PD)} & A_{22}^{(PD)} & 0 \\ 0 & 0 & A_{33}^{(PD)} \end{pmatrix} \begin{pmatrix} r_{ix} \\ r_{iy} \\ r_{iz} \end{pmatrix} + \begin{pmatrix} B_1^{(PD)} \\ B_2^{(PD)} \\ B_3^{(PD)} \end{pmatrix}, \quad (34)$$

where

$$\begin{aligned}A_{11}^{(PD)} &= \cos(2\omega_0 t) e^{-(R+2\gamma_{PD})t}, & A_{12}^{(PD)} &= -\sin(2\omega_0 t) e^{-(R+2\gamma_{PD})t}, \\ A_{21}^{(PD)} &= \sin(2\omega_0 t) e^{-(R+2\gamma_{PD})t}, & A_{22}^{(PD)} &= \cos(2\omega_0 t) e^{-(R+2\gamma_{PD})t}, & A_{33}^{(PD)} &= e^{-pRt}, \\ B_1^{(PD)} &= \frac{e^{-(R+2\gamma_{PD})t} pR \sin \eta (R + 2\gamma_{PD}) [e^{(R+2\gamma_{PD})t} \cos \zeta - \cos(\zeta + 2\omega_0 t)]}{(R + 2\gamma_{PD})^2 + 4\omega_0^2} \\ &\quad + \frac{e^{-(R+2\gamma_{PD})t} pR \sin \eta 2\omega_0 [-e^{(R+2\gamma_{PD})t} \sin \zeta + \sin(\zeta + 2\omega_0 t)]}{(R + 2\gamma_{PD})^2 + 4\omega_0^2}, \\ B_2^{(PD)} &= \frac{e^{-(R+2\gamma_{PD})t} pR \sin \eta (R + 2\gamma_{PD}) [e^{(R+2\gamma_{PD})t} \sin \zeta - \sin(\zeta + 2\omega_0 t)]}{(R + 2\gamma_{PD})^2 + 4\omega_0^2} \\ &\quad + \frac{e^{-(R+2\gamma_{PD})t} pR \sin \eta 2\omega_0 [e^{(R+2\gamma_{PD})t} \cos \zeta - \cos(\zeta + 2\omega_0 t)]}{(R + 2\gamma_{PD})^2 + 4\omega_0^2}, \\ B_3^{(PD)} &= (-e^{-pRt} + 1) \cos \eta.\end{aligned}\quad (35)$$

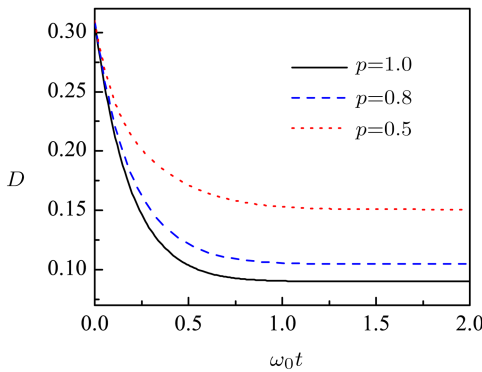


Fig. 7 (Color online) The trace distances as functions of the scaled time $\omega_0 t$ for different p under the PD channel: $p = 1$ (black solid line), $p = 0.8$ (blue dashed line) and $p = 0.5$ (red dotted line). The other parameters are $\gamma_{PD} = 0.1$, $R = 5$, $\eta = \pi/6$, $\zeta = 0$, and the initial parameters are $r_i = (1/2, 1/2, 1/2)^T$.

Comparing this solution (Eqs. (34) and (35)) with that of perfect feedback scheme (Eqs. (15) and (16)), we can see clearly that the feedback efficiency p affects the preparation process. The effect of feedback inefficiencies are shown in Fig. 7 where the trace distance are plotted as functions of the scaled time $\omega_0 t$ with different p . From Fig. 7, we can see that larger p will lead to the decrease of

trace distance, which stands for better preparation effect. Taking the missing of effective feedback control into account will make the effects of preparation and protection get worse. However, when p is large enough, this variation of trace distance is small, which means that as long as p is not small, our feedback control scheme can still be very effective.

6 Summary

In this paper, based on quantum trajectory theory, we have obtained an extended master equation for the dynamics of the reduced system under measurement and feedback control. Two prototypical classes of decoherence channels have been considered: phase damping channel and generalized amplitude damping channel. And for a two-level open system, we have obtained the exact analytic solution for the state vector dynamics. Using our explicit forms of the state vector dynamics, we have proposed some simple and effective measurement-based feedback control schemes which can drive any initial states to an arbitrary pure state under both PD and AD channels. Comparing the preparing effects under two kinds of noise channels, we have found that the effect of our measurement-based feedback control scheme under the PD channel is better than that under the AD channel, especially for severer environment noise. We have also considered a qubit initially prepared in one of two nonorthogonal states, and used

measurement and feedback control to stabilize it with high fidelity against decoherence. Through our study, we have demonstrated that projective measurement with unbiased basis is not always optimal for the protection task, and for both PD and AD channels, the effects of the optimal protection strongly depend on the initial states. Generally, the feedback scheme based on the weak measurement with

the best-biased basis could realize the best stabilization of two nonorthogonal states. Considering the amount of increase between our optimal measurement-based feedback control scheme and do-nothing, our protection schemes under the AD channel have better protective effect than that under the PD channel. We also discuss the inefficiencies in the feedback process.

References

- [1] E.B. Davies, *Quantum Theory of Open Systems*, Academic Press, London (1976).
- [2] H.P. Breuer and F. Petruccione, *The Theory of Open Quantum Systems*, Oxford University Press, Oxford (2007).
- [3] M.A. Nielson and I.L. Chuang, *Quantum Computation and Quantum Information*, Cambridge University Press, Cambridge (2000).
- [4] H.M. Wiseman and G.J. Milburn, Phys. Rev. Lett. **70** (1993) 548.
- [5] H.M. Wiseman, Phys. Rev. A **49** (1994) 2133.
- [6] W.P. Smith, J.E. Reiner, L.A. Orozco, S. Kuhr, and H.M. Wiseman, Phys. Rev. Lett. **89** (2002) 133601.
- [7] M.A. Armen, J.K. Au, J.K. Stockton, A.C. Doherty, and H. Mabuchi, Phys. Rev. Lett. **89** (2002) 133602.
- [8] M.D. Lahaye, O. Buu, B. Camarota, and K.C. Schwab, Science **304** (2004) 74.
- [9] H. Mabuchi and P. Zoller, Phys. Rev. Lett. **76** (1996) 3108.
- [10] D.B. Horoshko and S. Ya. Kilin, Phys. Rev. Lett. **78** (1997) 840.
- [11] A.C. Doherty and K. Jacobs, Phys. Rev. A **60** (1999) 2700.
- [12] A.C. Doherty, S. Habib, K. Jacobs, H. Mabuchi, and S.M. Tan, Phys. Rev. A **62** (2000) 012105.
- [13] A.N. Korotkov, Phys. Rev. B **63** (2001) 115403.
- [14] A.N. Korotkov, Phys. Rev. B **71** (2005) 201305(R).
- [15] H.M. Wiseman, S. Mancini, and J. Wang, Phys. Rev. A **66** (2002) 013807.
- [16] H.M. Wiseman and A.C. Doherty, Phys. Rev. Lett. **94** (2005) 070405.
- [17] C.W. Helstrom, *Quantum Detection and Estimation Theory*, Academic Press, New York (1976).
- [18] H.M. Wiseman, Phys. Rev. Lett. **75** (1995) 4587.
- [19] D.W. Berry and H.M. Wiseman, Phys. Rev. Lett. **85** (2000) 5098.
- [20] J.I. Cirac and P. Zoller, Phys. Rev. Lett. **74** (1995) 4091.
- [21] B.E. Kane, Nature (London) **393** (1998) 133.
- [22] P.O. Boykin, T. Mor, V. Roychowdhury, F. Vatan, and R. Vrijen, Proc. Natl. Acad. Sci. USA **99** (2002) 3388.
- [23] D.J. Tannor and A. Bartana, J. Phys. Chem. A **103** (1999) 10359.
- [24] S.E. Sklarz, D.J. Tannor, and N. Khaneja, Phys. Rev. A **69** (2004) 053408.
- [25] F. Verstraete, M. Wolf, and J.I. Cirac, Nat. Phys. **5** (2009) 633.
- [26] B. Kraus, H.P. Büchler, S. Diehl, A. Kantian, A. Micheli, and P. Zoller, Phys. Rev. A **78** (2008) 042307.
- [27] K. Jacobs, Phys. Rev. A **67** (2003) 030301(R).
- [28] J. Combes and K. Jacobs, Phys. Rev. Lett. **96** (2006) 010504.
- [29] H.M. Wiseman and J.F. Ralph, New J. Phys. **8** (2006) 90.
- [30] J. Combes, H.M. Wiseman, K. Jacobs, and A.J. O'Connor, Phys. Rev. A **82** (2010) 022307.
- [31] C.H. Bennett, Science **257** (1992) 752.
- [32] G.G. Gillett, R.B. Dalton, B.P. Lanyon, M.P. Almeida, M. Barbieri, G.J. Pryde, J.L. O'Brien, K.J. Resch, S.D. Bartlett, and A.G. White, Phys. Rev. Lett. **104** (2010) 080503.
- [33] A.M. Brańczyk, P.E.M.F. Mendonca, A. Gilchrist, A.C. Doherty, and S.D. Bartlett, Phys. Rev. A **75** (2007) 012329.
- [34] Y. Yang, X.Y. Zhang, J. Ma, and X.X. Yi, Phys. Rev. A **87** (2013) 012333.
- [35] Y. Yan, J. Zou, B.M. Xu, J.G. Li, and B. Shao, Phys. Rev. A **88** (2013) 032320.
- [36] H.M. Wiseman and G.J. Milburn, *Quantum Measurement and Control*, Cambridge University Press, Cambridge (2009).
- [37] Á. Rivas and S.F. Huelga, *Open Quantum Systems: An Introduction*, Springer, Heidelberg (2011).
- [38] G. Lindblad, Commun. Math. Phys. **48** (1976) 119.
- [39] J.D. Cresser, S.M. Barnett, J. Jeffers, and D.T. Pegg, Opt. Commun. **264** (2006) 352.
- [40] A. Steane, Rep. Prog. Phys. **61** (1998) 117.
- [41] D. Bouwmeester, A.K. Ekert, and A. Zeilinger, *The Physics of Quantum Information: Quantum Cryptography, Quantum Teleportation, Quantum Computation*, Springer, New York (2000).
- [42] K.A. Valiev, Phys. Usp. **48** (2005) 1.
- [43] J. Audretsch, T. Konrad, and A. Scherer, Phys. Rev. A **63** (2001) 052102.
- [44] A. Acín, E. Bagan, M. Baig, L. Masanes, and R.M. Tapia, Phys. Rev. A **71** (2005) 032338.